Landes Bioscience www.landesbioscience.com

Supplemental Material to:

Ping-Hung Chen, Fan-Ching Chien, Sue-Ping Lee, Woan-Eng Chan, I-Hsuan Lin, Chun-Shan Liu, Fang-Jen Lee, Jiann-Shiun Lai, Peilin Chen, Hsin-Fang yang-yen and Jeffrey Jong-Young Yen

Identification of a novel function of the clathrin-coated structure at the plasma membrane in facilitating GM-CSF receptor-mediated activation of JAK2

2012; 11(19)
http://dx.doi.org/10.4161/cc.21920

http://www.landesbioscience.com/journals/cc/article/21920

Supplemental Materials and Methods

Preparation of Fab fragments recognizing human GMRα and GMRβ

Antibodies specific to human GMRα (CD116, clone 4H1) and GMRβ (CD131, clone 1C1) (eBioscience, CA, USA) were digested with papain, followed by running through the protein G-Sepharose CL-4B column (GE, Piscataway, NJ, USA) to remove the Fc fragments. The flow-through fraction that contains the Fab fragment was concentrated by using the Sephacry S-200 column (GE) according to the standard protocol. Purified Fab fragments recognizing GMRα or GMRβ were subsequently labeled with fluorochrome using Alexa Fluor® 488 protein labeling kit (Invitrogen, Grand Island, NY) or EasyLink-Cy5 conjugation kit (Abcam, Cambridge, MA, USA), respectively.

Photoactivated localization microscopy (PALM) analysis

To investigate the distribution of GMRβ−paGFP molecules on the plasma membrane (**Fig. S1A**), HeLa cells transiently co-expressing GMRα-CFP and GMRβ−paGFP were treated or not treated with GM-CSF, and visualized under the TIRF microscope with CFP channel to select GMRα-positive cells for further PALM analysis. In PALM imaging acquisition, a solid-state laser (Changchun New Industries Optoelectronics Tech) with a wavelength of 405 nm (100 mW) was added to the dSTROM system as

the activation light source. To acquire the fluorescence image stacks, a few of pa-GFP fusion proteins were activated stochastically by the activation light. Then, the fluorescence signals from single pa-GFP molecules were recorded by the excitation light source with a wavelength of 473 nm. The fluorescence image stacks were collected by repeating the photo-activation and fluorescence read-out sequences. Finally, after localizing the centroids of individual molecules and image reconstruction, the PALM images of GMRβ-paGFP were obtained. The size of receptor cluster and number of receptor molecules in a cluster were calculated as described in the text.

FigS1

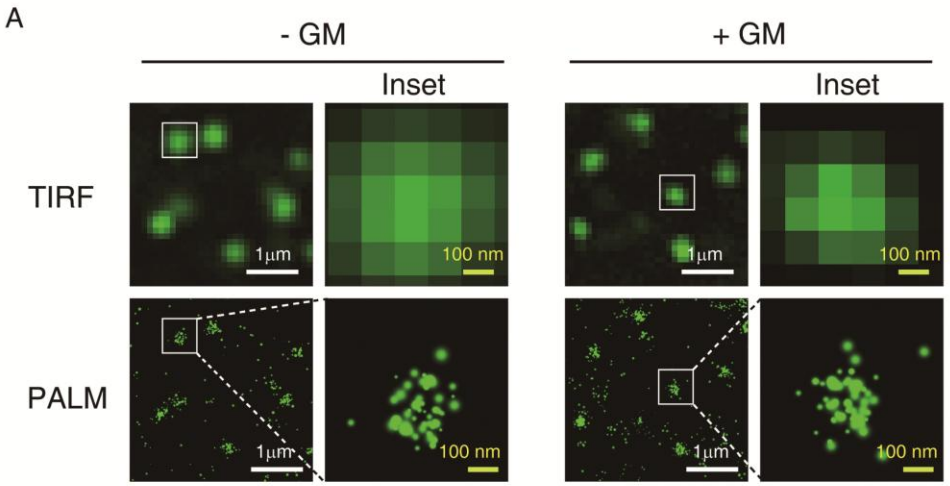
A
- GM
+ GM
Inset
Inset
TIRF
PALM
1μm
100 nm
1μm
100 nm
1μm
100 nm
1μm
100 nm

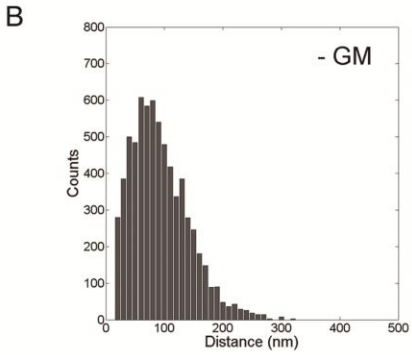
B
- GM
Counts
Distance (nm)

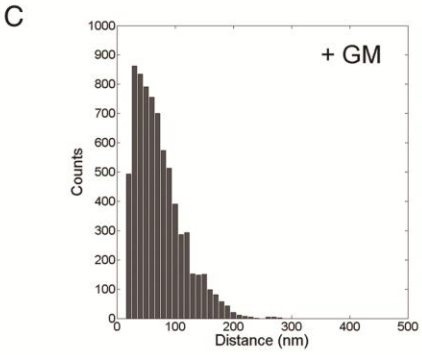
C
+ GM
Counts
Distance (nm)

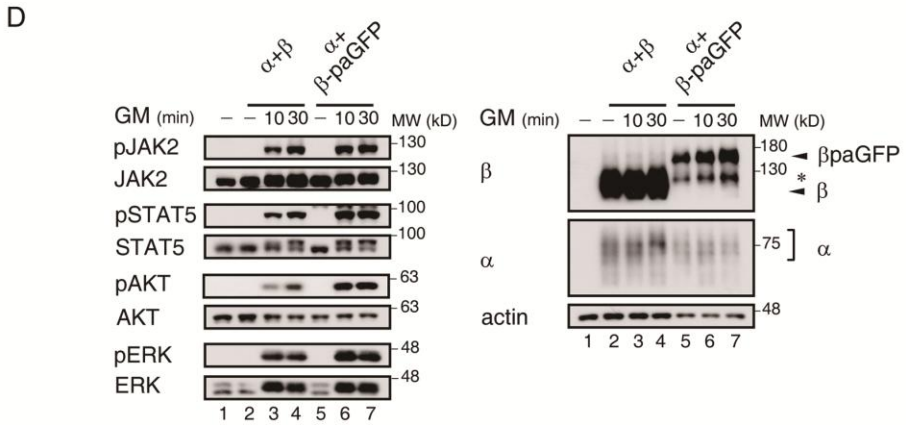
D
α+β
α+ β-paGFP
GM (min)
MW (kD)
pJAK2
JAK2
pSTAT5
STAT5
pAKT
AKT
pERK
ERK
1 2 3 4 5 6 7
β
α
actin
βpaGFP
β

Figure S1. Surface GMRβ-paGFP molecules form ligand-independent nano-scale clusters. (A) TIRF and PALM images of GMRβ-paGFP clusters in HeLa cells transiently co-expressing GMRα-CFP (not shown) and GMRβ-paGFP in medium containing or not containing GM-CSF (±GM). (B) and (C) are representative pair distance histograms of GMRβ-paGFP proteins within a GMRβ-paGFP cluster shown in (A) calculated by protein pair distance correlation analysis. According to the distance histograms, the size of a GMRβ-paGFP cluster without or with ligand treatment are 202.85 ± 69.51 nm and 199.68 ± 67.93 nm, respectively. The average number of GMRβ-paGFP molecules in GMRβ-paGFP clusters without or with ligand treatment are 53.58 ± 15.74 and 53.40 ± 26.09, respectively. (n=50). (D) GMRβ-paGFP transduces signals like the wt protein. HeLa cells transiently co-expressing GMRα (α) and wt GMRβ (β) or GMRβ-paGFP (β-paGFP) were left untreated (-) or stimulated with hGM-CSF (10ng/ml) for 10 or 30 minutes. The cell lysates, resolved on two different membranes (left and right panels), were analyzed by immunoblotting using antibodies specific to each indicated molecule.

FigS2

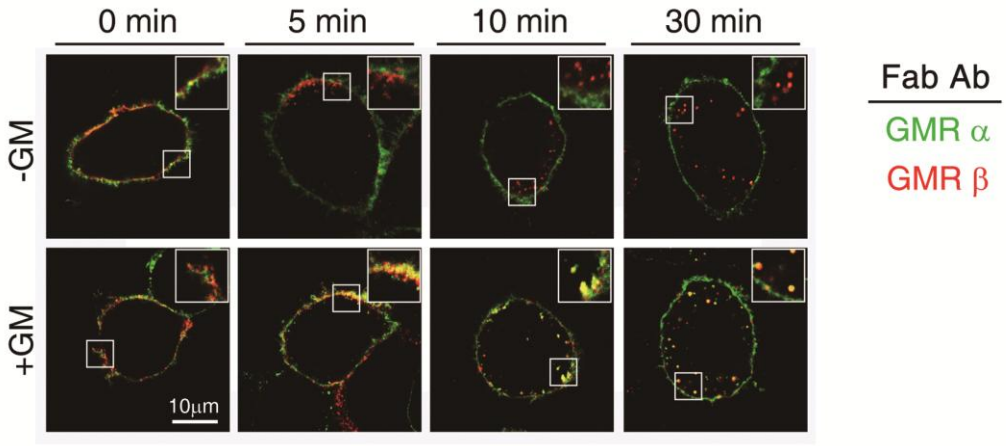

Figure S2. Ligand-dependent co-internalization of GMRα with GMRβ revealed by the internalization assay using the Fab fragments of GMRα and GMRβ antibodies. HeLa cells transiently co-expressing GMRα and GMRβ were pre-labeled with Alexa Fluor® 488-conjugated Fab fragment recognizing GMRα (green) and Cy5-conjugated Fab fragment recognizing GMRβ (red) at 4°C for 30 min. Receptor endocytosis was then initiated by transferring these antibody-labeled cells to 37°C in medium containing or not containing GM-CSF (±GM). At various time points (0-30 min) after receptor endocytosis had started, cells were immediately shifted back to 4°C, fixed with 4% paraformaldehyde and the extent of receptor internalization was analyzed by confocal microscopy.

FigS3

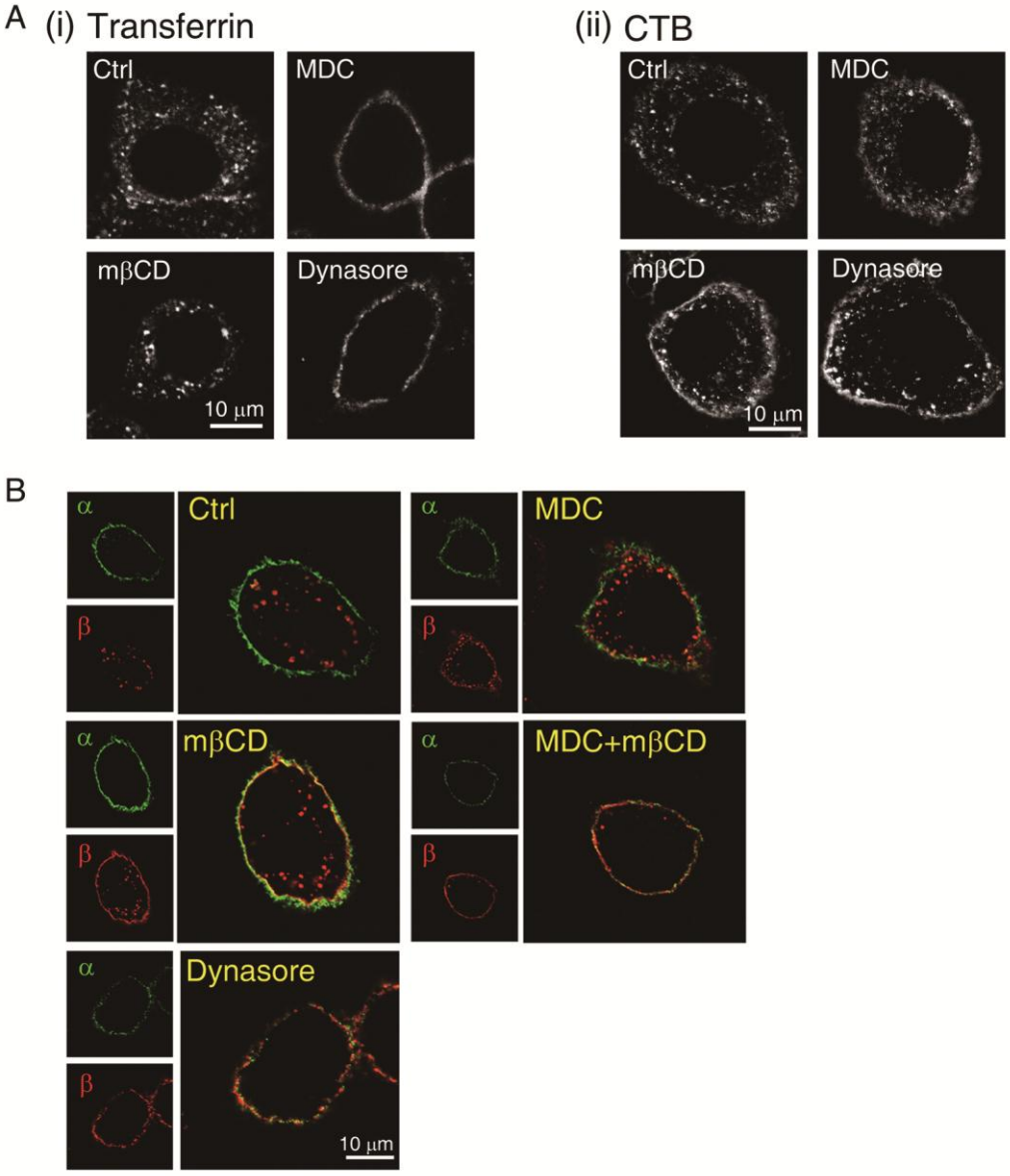

Figure S3. (A) Specificity of various endocytic pathway inhibitors. Endocytosis of Alexa Flour®633 conjugated transferrin (i) or Alexa Flour®555 conjugated cholera toxin subunit B (CTB) (ii) in HeLa cells was allowed to proceed for 15 min at 37℃ in the presence of the indicated inhibitors. (B) Unliganded GMRβ is endocytosed via both clathrin- and lipid raft-dependent pathways. The endocytosis of unliganded

receptor was allowed to proceed in HeLa cells transiently co-expressing GMRα (green) and GMRβ (red) in the presence of the indicated endocytosis inhibitors essentially as that described in the legend to Figure 2C in the text except that cells were placed in ligand-free medium during the endocytosis step.

FigS4

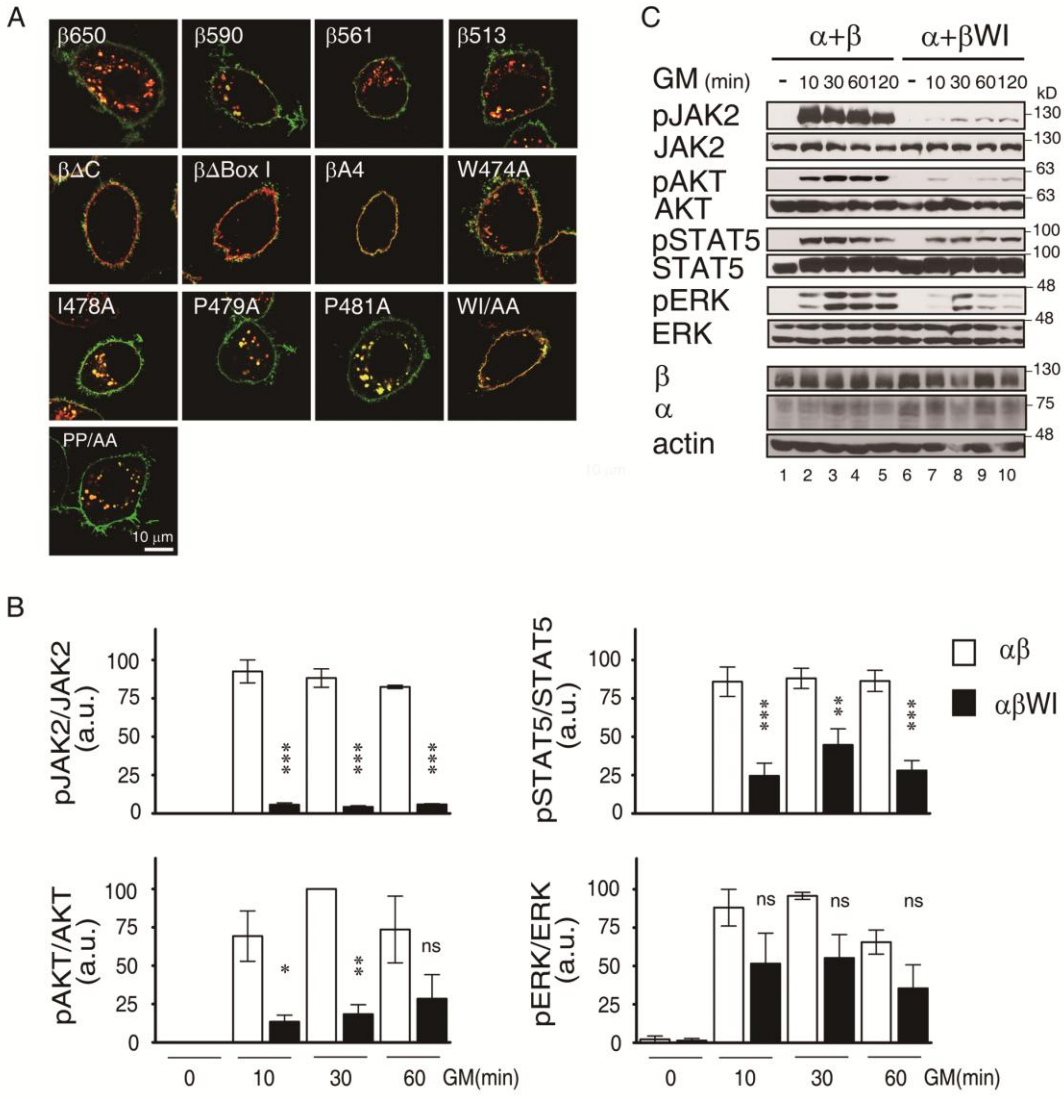

Figure S4. The WI/AA mutation impairs GMR internalization and signaling.

(A) The internalization assay was performed with HeLa cells transiently co-expressing GMRα (green) and each GMRβ mutant as indicated (red). After 30 min in medium containing GM-CSF, cells were processed and analyzed by confocal microscope. (B) The activation (phosphorylation) extent of JAK2 and AKT in αβ- and αβWI-Ba/F3 cells shown in Fig. 3F of the text plus very similar results from two other independent experiments was quantified and plotted essentially as that described

in the Materials and methods. *, $p<0.05$; ** $p<0.01$; *** $p<0.001$. n.s., no statistical difference. (C) HeLa cells transiently co-expressing GMRα and wt or the WI/AA mutant of GMRβ were left untreated (-) or stimulated with hGM-CSF (10ng/ml) for various time points as indicated. The cell lysates were analyzed by immunoblotting using antibodies specific to each indicated molecule.

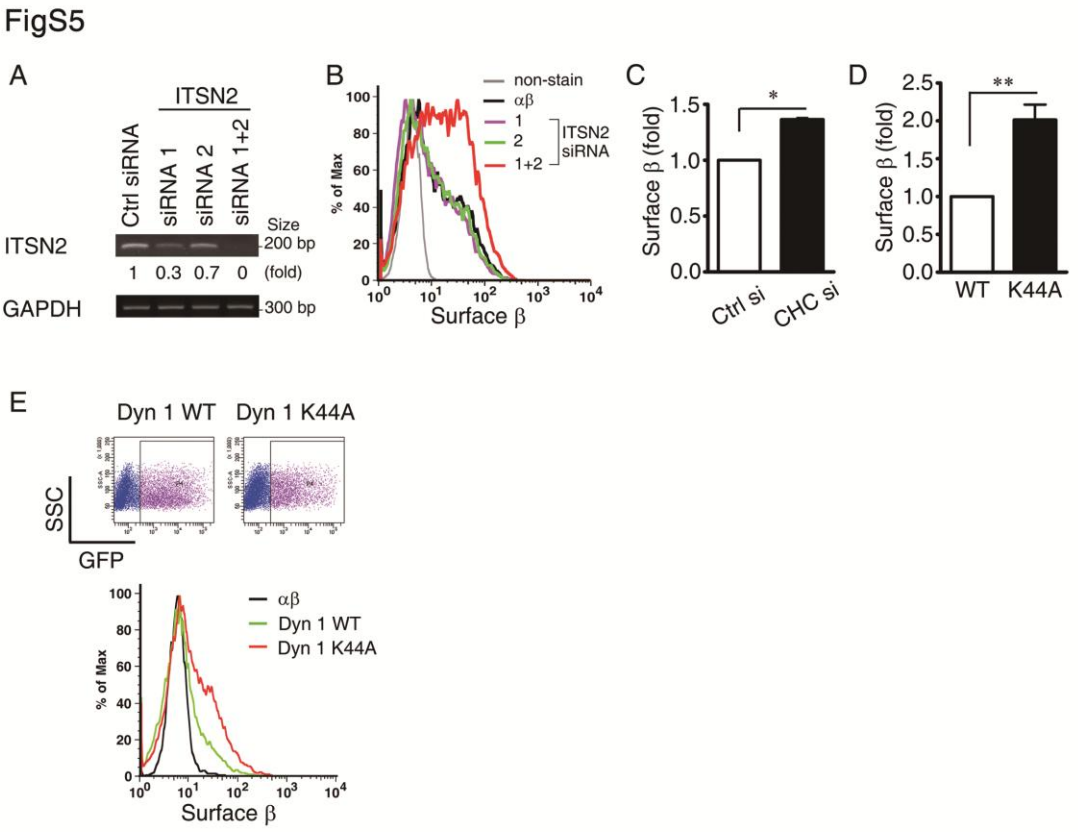

Figure S5. Interference of clathrin-mediated endocytosis inhibits GMRβ internalization. (A) The ITSN2 mRNA levels in control and ITSN2 knockdown (with siRNA1, siRNA2 or the combination of both) αβ-Ba/F3 cells were determined by semi-quantitative RT-PCR. (B-D) Flow cytometric analysis of cell surface levels of GMRβ in control, ITSN2 or CHC knockdown αβ-Ba/F3 cells or in αβ-Ba/F3 cells transiently expressing wt or the K44A mutant of dynamin I. Data shown (mean ± SEM, n=3) are relative protein levels compared to that of the control cells. ∗ $p<0.05$; ∗∗, $p<0.01$. (E) Representative FACS profiles of dynamin I-GFP fusion proteins and surface expression of GMRβ in control or in αβ-Ba/F3 cells transiently expressing wt or the K44A mutant of dynamin I. Similar number of GFP positive cells were sorted

out from αβ-Ba/F3 cells transiently expressing wt or the K44A mutant of dynamin I for immunoblotting analysis shown in Fig. 4H of the text.